Environmental Research 179 (2019) 108798

Contents lists available at ScienceDirect

Environmental Research

journal homepage: www.elsevier.com/locate/envres

# Assessment of the potential for in-plume sulphur dioxide gas-ash interactions to influence the respiratory toxicity of volcanic ash

Ines Tomašek[a,b,1,*], David E. Damby[c], Claire J. Horwell[a], Paul M. Ayris[d], Pierre Delmelle[e], Christopher J. Ottley[f], Pablo Cubillas[f], Ana S. Casas[d], Christoph Bisig[b,2], Alke Petri-Fink[b,g], Donald B. Dingwell[d], Martin J.D. Clift[h], Barbara Drasler[b], Barbara Rothen-Rutishauser[b]

[a] Institute of Hazard, Risk and Resilience, Department of Earth Sciences, Durham University, Science Labs, Durham, DH1 3LE, United Kingdom
[b] BioNanomaterials, Adolphe Merkle Institute, University of Fribourg, Chemin des Verdiers 4, CH-1700, Fribourg, Switzerland
[c] Volcano Science Center, United States Geological Survey, Menlo Park, California, 94025, United States
[d] Department of Earth and Environmental Sciences, Section for Mineralogy, Petrology and Geochemistry, Ludwig-Maximilians-Universität München, Theresienstrasse 41, D-80333, Munich, Germany
[e] Earth & Life Institute, Université catholique de Louvain, Croix Du Sud 2, 1348, Louvain-la-Neuve, Belgium
[f] Department of Earth Sciences, Durham University, Science Labs, Durham, DH1 3LE, United Kingdom
[g] Chemistry Department, University of Fribourg, Chemin des Musee, CH-1700, Fribourg, Switzerland
[h] In Vitro Toxicology Group, Swansea University Medical School, Singleton Park Campus, Swansea, SA2 8PP, United Kingdom

ARTICLE INFO

*Keywords:*
Volcanic ash
Sulphur dioxide
Leaching
Respiratory hazard
Multicellular lung model

ABSTRACT

*Background:* Volcanic plumes are complex environments composed of gases and ash particles, where chemical and physical processes occur at different temperature and compositional regimes. Commonly, soluble sulphate- and chloride-bearing salts are formed on ash as gases interact with ash surfaces. Exposure to respirable volcanic ash following an eruption is potentially a significant health concern. The impact of such gas-ash interactions on ash toxicity is wholly un-investigated. Here, we study, for the first time, whether the interaction of volcanic particles with sulphur dioxide ($SO_2$) gas, and the resulting presence of sulphate salt deposits on particle surfaces, influences toxicity to the respiratory system, using an advanced *in vitro* approach.

*Methods:* To emplace surface sulphate salts on particles, *via* replication of the physicochemical reactions that occur between pristine ash surfaces and volcanic gas, analogue substrates (powdered synthetic volcanic glass and natural pumice) were exposed to $SO_2$ at 500 °C, in a novel Advanced Gas-Ash Reactor, resulting in salt-laden particles. The solubility of surface salt deposits was then assessed by leaching in water and geochemical modelling. A human multicellular lung model was exposed to aerosolised salt-laden and pristine (salt-free) particles, and incubated for 24 h. Cell cultures were subsequently assessed for biological endpoints, including cytotoxicity (lactate dehydrogenase release), oxidative stress (oxidative stress-related gene expression; heme oxygenase 1 and NAD(P)H dehydrogenase [quinone] 1) and its (pro-)inflammatory response (tumour necrosis factor α, interleukin 8 and interleukin 1β at gene and protein levels).

*Results:* In the lung cell model no significant effects were observed between the pristine and $SO_2$-exposed particles, indicating that the surface salt deposits, and the underlying alterations to the substrate, do not cause acute adverse effects *in vitro*. Based on the leachate data, the majority of the sulphate salts from the ash surfaces are likely to dissolve in the lungs prior to cellular uptake.

*Conclusions:* The findings of this study indicate that interaction of volcanic ash with $SO_2$ during ash generation

* Corresponding author: Analytical, Environmental and Geochemistry group (AMGC), Department of Chemistry and Physical Geography group (FARD), Department of Geography, Vrije Universiteit Brussel, Pleinlaan 2, B-1050, Brussel, Belgium.
*E-mail address:* ines.tomasek@vub.be (I. Tomašek).
[1] Present address: Analytical, Environmental and Geochemistry group, Department of Chemistry and Physical Geography group, Department of Geography, Vrije Universiteit Brussel, Pleinlaan 2, B-1050 Brussel, Belgium.
[2] Present address: Cooperation Group of Comprehensive Molecular Analytics, Helmholtz Zentrum München, German Research Center for Environmental Health (GmbH), Gmunderstraβe 37, D-81379 Munich, Germany.

https://doi.org/10.1016/j.envres.2019.108798
Received 12 March 2019; Received in revised form 9 September 2019; Accepted 4 October 2019
Available online 05 October 2019

and transport does not significantly affect the respiratory toxicity of volcanic ash *in vitro*. Therefore, sulphate salts are unlikely a dominant factor controlling variability in *in vitro* toxicity assessments observed during previous eruption response efforts.

**List of abbreviations**

| | |
|---|---|
| AGAR | Advanced Gas-Ash Reactor |
| ALI | Air-liquid interface |
| $CaSO_4$ | Calcium sulphate |
| *CASP7* | Caspase-7 gene |
| cRPMI | Complete RPMI 1640 cell medium (supplemented with 1 % L-Glutamine, 1 % Penicillin/Streptomycin and 10 % fetal bovine serum) |
| *FAS* | FAS receptor gene |
| *GAPDH* | Glyceraldehyde-3-phosphate dehydrogenase gene |
| G_CTRL | Control volcanic glass (exposed to Ar in AGAR) |
| G_$SO_2$ | Salt-laden volcanic glass (exposed to $SO_2$ in AGAR) |
| *HMOX1* | Heme oxygenase 1 gene |
| IL-1β | Interleukin 1 beta protein |
| *IL1B* | Interleukin 1 beta gene |
| IL-8 | Interleukin 8 protein |
| *IL8* | Interleukin 8 gene |
| LDH | Lactate dehydrogenase |
| LSM | Laser scanning microscopy |
| MDDC | Monocyte-derived dendritic cells |
| MDM | Monocyte-derived macrophages |
| *NQO1* | NAD(P)H dehydrogenase [quinone] 1 gene |
| P_CTRL | Control pumice (exposed to Ar in AGAR) |
| P_$SO_2$ | Salt-laden pumice (exposed to $SO_2$ in AGAR) |
| PBS | Phosphate buffered saline |
| PET | Polyethylene terephthalate |
| PSD | Particle size distribution |
| QCM | Quartz crystal microbalance |
| qRT-PCR | Quantitative reverse-transcriptase polymerase chain reaction |
| mRNA | Messenger ribonucleic acid |
| ROS | Reactive oxygen species |
| SCCM | Standard cubic centimeters per minute |
| SEM | Scanning electron microscopy |
| SI | Saturation index |
| $SiO_2$ | Silicon dioxide |
| $SO_2$ | Sulphur dioxide |
| TNF-α | Tumour necrosis factor alpha |

## 1. Introduction

Volcanic plumes are complex environments composed of gases and ash particles, where various chemical and physical processes occur in different compositional regimes over a spectrum of temperatures (ranging from magmatic to atmospheric) and timescales (seconds to days). Gas adsorption onto the surface of ash particles, together with associated subsequent chemical reactions, leads to scavenging of volatiles (such as sulphur and halogen gases and metals), whereby these components are removed from the atmosphere, commonly in the form of salts with various solubilities, which grow on the ash surfaces (Witham et al., 2005; Ayris and Delmelle, 2012). These are believed to consist of various sulphates and halides, including $CaSO_4$, $Na_2SO_4$, NaCl, NaF, $CaCl_2$, $CaF_2$, $K_2SiF_6$, $Na_2SiF_6$ and $AlF_3$ (Cronin et al., 2003; de Moor et al., 2005; Delmelle et al., 2007; Gislason et al., 2011). The salts can be emplaced onto the ash particles from the aerosol formed by degassing volatiles at magmatic temperatures (600–1200 °C) (Smith et al., 1982, 1983; Taylor and Stoiber, 1973) or be formed by heterogeneous reactions (*e.g.*, chemisorption) between gases and ash particle surfaces at intermediate temperatures (300–700 °C) (Ayris et al., 2013, 2014; Hoshyaripour et al., 2014; Oskarsson, 1980). Salts can also precipitate due to partial leaching and dissolution of ash particles by acidic condensates (*e.g.*, $H_2SO_4$, HCl and HF) in the cold volcanic cloud (< 190 °C) (Mueller et al., 2017; Delmelle et al., 2007; Rose, 1977). Following an eruption, these species are then transported on the ash and dispersed into the environment. Depending on the size of an eruption and wind speed, ash deposition may be limited to the proximal area around the volcano or it can be transported and dispersed over a more extensive area (*e.g.*, the 2010 eruption of Eyjafjallajökull volcano, Iceland resulted in an increase in ambient particulate over a large part of Europe (Gudmundsson et al., 2012)), consequently having various impacts on the receiving natural and human environments (Ayris and Delmelle, 2012; Barsotti et al., 2010), including potential adverse effects on human health (Baxter, 2000).

Whilst the effects of chronic exposure are still largely unknown (Hincks et al., 2006; Buist et al., 1986), acute exposure to respirable volcanic ash has been associated with an exacerbation of pre-existing respiratory diseases, such as asthma and bronchitis (Baxter et al., 1983). In addition, increases in hospital and emergency department admissions due to respiratory problems, such as irritation and cough, are documented to have been associated with ashfall events (Carlsen et al., 2012; Baxter et al., 1981). The incidence of such acute respiratory symptoms following an eruption, however, has been inconsistent, likely due to different physicochemical properties of ash, varying exposure concentrations and documentation of symptoms (see review in Kar-Purkayastha et al. (2012)). Similarly, toxicology assessments for volcanic ash have shown high variability in discrete results, generally concluding that ash causes low toxicity *in vitro* and *in vivo*, although various studies have demonstrated the potential of ash to induce inflammatory immune responses (Damby et al., 2013, 2016, 2018; Horwell et al., 2013; Monick et al., 2013; Lee and Richards, 2004). Studies on volcanic ash toxicity have often focused on the crystalline silica content, mainly in the form of cristobalite (Bérubé et al., 2004; Horwell et al. (2003a)), and reactive surface iron (Horwell et al. (2003b), 2007) due to their known potential to drive adverse reactions that may result in the development, or exacerbation, of lung diseases. However, mechanisms involved in any observed ash toxicity are still poorly constrained (Damby et al., 2017; Horwell et al., 2012; Nattrass et al., 2017).

The potential impact of surface salts on the respiratory toxicity of volcanic ash is, to date, unknown. This is despite the fact that their presence is likely to be common, yet variable in extent, such that it could be a hitherto unexplored controlling factor in toxicity (either augmenting or reducing it). Leachable components on particle surfaces, as well as the underlying chemical functionalities at the surface, are known to have an important role in driving adverse respiratory health effects following exposure to ambient particles (*e.g.*, Gilmour et al., 1996, Carter et al., 1997, Fubini et al., 1995, Rice et al., 2001, Fubini, 1997). For example, particles containing chelatable metals are known for their potential to induce oxidative stress *via* free radical generation in the biological environment and upon contact with biological structures, and have also been found to stimulate the release of (pro-)inflammatory markers (Cho et al., 2010, 2012; Smith et al., 2000). For volcanic ash, it has been postulated that soluble compounds adsorbed on ash, if leached from the particle surface, could be a potential cause, at least in part, of reported irritancy to the eyes, throat and airways following exposure to ash (Horwell and Baxter, 2006; Searl et al., 2002; Witham et al., 2005; Hansell et al., 2006).

Freshly erupted volcanic ash surfaces are composed of heterogeneously distributed chemically reactive surface sites, including

acidic, basic, reduced and oxidised sites in various proportions (Maters et al., 2016). The nature and abundance of such reactive sites on particle surfaces are likely being modulated during ash transport through the eruption plume, as these sites readily react with gases and aerosols (Ayris et al., 2013, 2014), thus resulting in the formation of surface deposits (salts) but, also, potential changes to ash surface physico-chemical properties and reactivity. Thus, the potential consequences of such in-plume processing may augment the toxic potential of volcanic ash, but this has not been addressed in studies to date. The aim of the present study was, therefore, to investigate the biological impact of in-plume volatile scavenging on ash toxicity. To achieve this, a multi-cellular model mimicking the human lung epithelial tissue was exposed, at the air-liquid interface (ALI), to simulated respirable ash which was either salt-laden or pristine, in a constrained laboratory setting.

## 2. Materials and methods

Salt-laden particles were produced through simulated high-temperature in-plume processing using the Advanced -GasAsh Reactor (AGAR; see Section 2.1.2 for further detail of experimental setup) (Ayris et al., 2015). Samples were exposed to a single gas, sulphur dioxide ($SO_2$) as it is one of the principal gases released in abundance during volcanic activity, at a single temperature (500 °C), thus generating salt-laden particles in controlled conditions. This approach was based on previous experiments using the AGAR where silicate glasses with a range of representative volcanic compositions were exposed to $SO_2$ gas at high temperatures (Ayris et al., 2013). These experiments demonstrated that the uptake of $SO_2$ gas at and above 500 °C occurs *via* rapid adsorption onto reactive surface sites followed by the formation of calcium sulphate ($CaSO_4$) deposits at the particle surface (Ayris et al., 2013; Delmelle et al., 2018; Renggli and King, 2018). The experiments were conducted using two analogue substrates, pulverised synthetic volcanic glass and natural pumice, in order to obtain fresh particle surfaces which had not previously been exposed to gases in a volcanic plume. This model system was used since the reactive surface sites which may exist on natural, erupted ash may already have been filled or

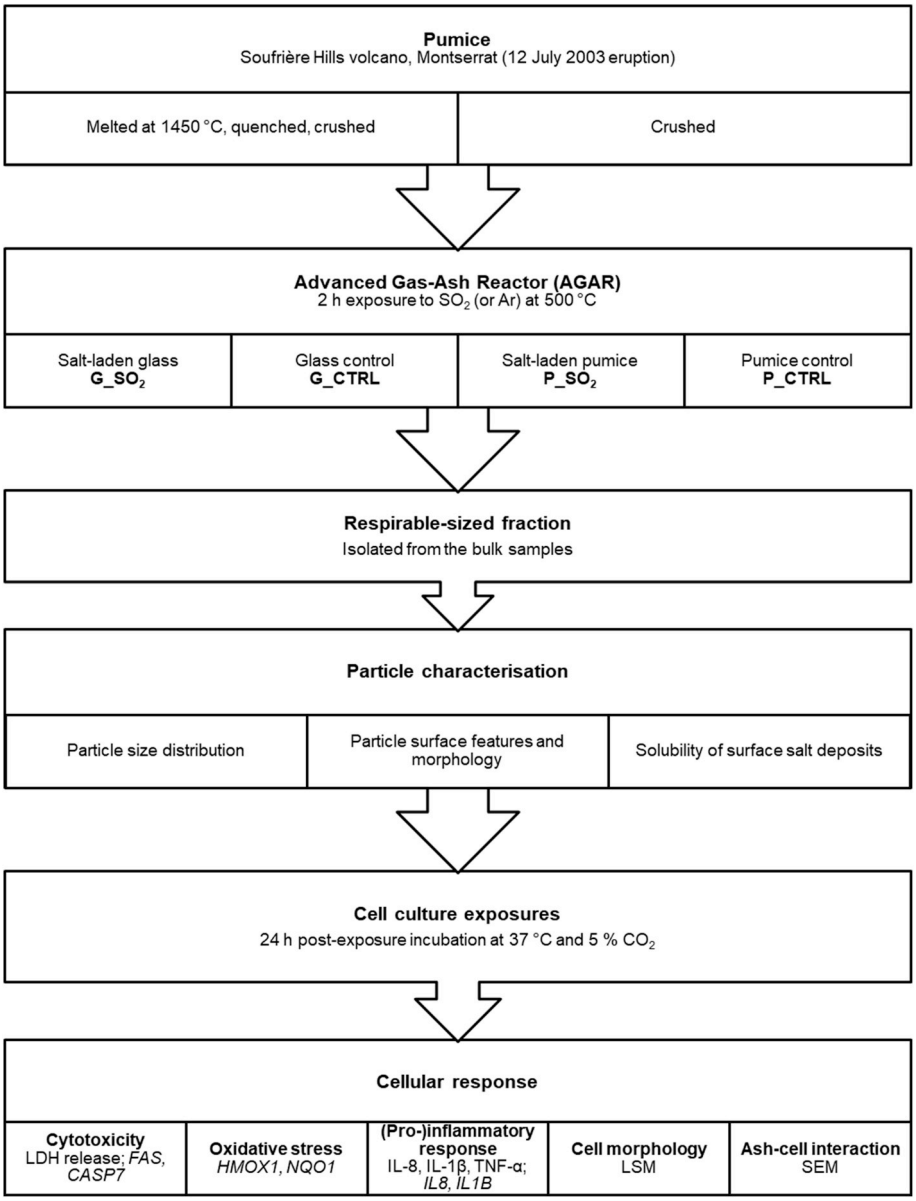


**Fig. 1. Schematic of the work-flow for the generation and exposure of analogue samples to sulphur dioxide ($SO_2$) gas in the Advanced Gas-Ash Reactor (AGAR) and subsequent use for hazard assessment *in vitro*.** Cell culture supernatant and membrane inserts were sampled at the 24 h time-point. Cell cultures were maintained under air-liquid interface (ALI) conditions throughout the duration of particle exposure experiments.

modified by in-plume transport and deposition and, thus, natural ash is not appropriate for the use in the AGAR experiments, nor for the toxicological assessment. The glass represents a homogenous proxy particle for the primary constituent of volcanic ash which allows assessment of the impact of surface changes without the additional effects of the natural substrate heterogeneity. Crushed pumice was used because it is representative of a real, multi-phase volcanic substrate, as was also used by Damby et al. (2018).

Respirable fractions of AGAR-exposed samples were isolated from the bulk samples for subsequent use in cell-based toxicity assessments. The isolated samples were characterised for their particle size, imaged to confirm the presence of surface salt deposits and solubility of the salts was measured. Cell cultures were assessed for biological endpoints relevant for common particle-induced toxicity mechanisms, including cytotoxicity (lactate dehydrogenase (LDH) release), oxidative stress (oxidative stress-related gene expression) and (pro-)inflammatory response (tumour necrosis factor α, interleukin 8 and interleukin 1β at gene (*IL8, IL1B*) and protein (TNF-α, IL-8, IL-1β) levels). The impact of particle exposures upon cell morphology as well as interaction with the multicellular model was visualised *via* confocal laser scanning microscopy (LSM) and scanning electron microscopy (SEM), respectively.

### 2.1. Particle generation, preparation and characterisation

#### 2.1.1. Analogue particle generation

Analogue materials were used as proxies for volcanic ash in this study instead of natural samples, which would have poorly constrained sample histories. These materials were crushed synthetic volcanic glass and natural pumice. The glass sample was synthetized by melting of a sample of andesitic pumice sourced from the Soufrière Hills volcano, Montserrat (from the 12 July 2003 eruption) at 1450 °C. The melt was homogenized and then rapidly quenched to produce glass, which was ground to a powder using an agate planetary ball mill. Pumice sourced from the same eruption was used to make an artificial ash sample by hand grinding the pumice to a powder using an agate pestle and mortar. These materials are fully characterised in Damby et al. (2018).

#### 2.1.2. Surface salt formation

The AGAR was used to simulate $SO_2$ gas uptake and surface-salt formation by volcanic glass and pumice, at the Ludwig Maximilian University of Munich, Germany. The instrument is composed of a horizontal tube furnace, loaded with a quartz glass tube fitted with a gas injector assembly at the tube inlet enabling delivery of a gas stream into the tube. The working tube can be rotated, enabling tumbling of material during the experiments for maximum surface-gas interaction. The details of the instrument design and operational conditions are described in Ayris et al. (2015).

In the present study, *ca.* 6 g of sample per experimental run was loaded into the quartz sample bulb and placed within the horizontal tube furnace and heated to a temperature of 500 °C. All experiments were carried out under a 25 SCCM (Standard Cubic Centimeters per Minute) gas stream of $SO_2$ and 75 SCCM of argon (Ar) carrier gas, exposing glass and pumice samples for a total of 120 min. Control samples for both materials were produced under a 100 SCCM Ar flow only, for 120 min.

After the experiment, samples were removed from the reactor and left to cool to ambient temperature, and then stored in sealed vials prior to their physical characterisation and the isolation of the respirable fraction. Experiments were conducted on three different occasions for each (final) particle type (Fig. 1) and then combined in order to maximise the amount of material available for the study.

#### 2.1.3. Isolation of the respirable fraction

Respirable-sized fractions were isolated from the pristine (Ar-exposed) and $SO_2$-exposed bulk samples using a Sioutas Cascade Impactor (*SKC Inc.,* USA) and Leland Legacy sample pump (*SKC Inc.,* USA) attached to a gravitational separation chamber, as previously described (Tomašek et al., 2016, 2018). Briefly, a sub-sample of post-AGAR volcanic glass or pumice was introduced into a gravitational separation chamber *via* an airstream (5 L/min) established by the pump. In the chamber, particles above a theoretical spherical aerodynamic diameter of 5 μm sedimented while the smaller particles were sampled by the impactor and, finally, recovered for further use.

#### 2.1.4. Physical characterisation of particles

The particle size distribution of isolated respirable samples was determined by a Beckman-Coulter LS230 laser particle analyser (*Coulter Corporation,* USA) in water without sonication, at the Ludwig Maximilian University of Munich, Germany. Results are the mean of three consecutive runs of each sample.

Observation and confirmation of particle size and surface salts were carried out on a JEOL JSM-6500F field emission scanning electron microscope (FE-SEM; *JEOL*, USA) at the HP-HT Laboratory of the National Institute of Geophysics and Volcanology (INGV) in Rome, Italy.

#### 2.1.5. Solubility of surface salt deposits

The concentrations of water-soluble elements from the experimental samples were assessed to identify the surface salt species formed during the AGAR experiments. In addition, the solubility of the salts over time was assessed in order to estimate if surface salts were likely to still be on the particles at the point of cellular uptake, so that toxicological data could be better interpreted.

For this purpose, 0.2 g of the post-AGAR (bulk) samples were leached with deionized water at a ratio of 1:100 (g dry weight ash to mL water) in three replicates (as recommended in Stewart et al. (2013)), each with a contact time of 1 h at room temperature without shaking. Additional tests were performed with contact times of 10 min and 30 min (one replicate each) to assess the rate of dissolution of salt deposits. Subsequently, subsamples of the leachates were filtered through 0.2 μm and 0.45 μm filters for anion and cation analysis, respectively. The concentrations of major cations (Ca, Mg, Na, K) and minor elements (Al, Fe, Mn, Zn, Cu) in collected extracts were measured by inductively coupled plasma-mass spectrometry (ICP-MS) at the Department of Earth Sciences, Durham University, UK. Anion analysis ($Cl^-$, $F^-$, $SO_4^{2-}$, $PO_4^{3-}$, $NO_3^-$) of water leachates was conducted by ion chromatography (IC) at the Department of Geography, Durham University, UK. The results are expressed in mg element per kg of dry sample weight.

To investigate if sulphate salts might oversaturate the solution when they leach from the particle surface in contact with the cell layer lining fluid in *in vitro* experiments, reaction-path modelling using PHREEQC software for Windows (Parkhurst and Appelo, 2013) was conducted. Simulations were performed by creating an aqueous solution with the given concentrations of different salts used to make a simulated lung fluid (SLF; *e.g.*, Gamble's solution) (Moss, 1979). This mimics the environment that particles would encounter following deposition in the lungs. In a second step, the measured water-leach concentrations (at 60 min time-point) for $SO_2$-exposed samples were added to the SLF solution (as $CaSO_4$, $Na_2SO_4$ and $MgSO_4$ salts). The saturation index (SI), a parameter determining whether a solution will tend to dissolve or precipitate a particular mineral based on the chemical activities of the dissolved ions of the mineral (ion activity product) with their solubility product, was automatically calculated and used to indicate whether sulphate salts dissolve ($SI < 0$) or precipitate ($SI > 0$) in the solution.

### 2.2. Cell cultures

Particle exposure experiments were performed using an established multicellular lung model mimicking the human alveolar epithelial tissue barrier (Rothen-Rutishauser et al., 2005, 2008; Blank et al., 2007), which has previously been applied to volcanic ash by the

authors (Tomašek et al., 2016, 2018). The model was composed of a layer of human alveolar type II-like epithelial cells (A549), combined with peripheral blood monocyte-derived macrophages (MDM) and dendritic cells (MDDC), cultured at the ALI.

A549 epithelial cells were cultured on 6-well cell culture inserts (polyethylene terephthalate (PET) membrane, 4.2 $cm^2$ growth area, 3.0 μm pore size; BD Falcon™, *BD Biosciences,* USA), seeded at a density of $1 \times 10^6$ cells/insert and maintained at 37 °C and 5 % $CO_2$ for 5 days prior to the addition of immune cells to form a co-culture. For each exposure, human blood monocytes were isolated from different, individual buffy coats (provided by the Transfusion Blood Bank; *Blutspendedienst SRK Bern AG*, Switzerland), using $CD14^+$ magnetic beads (MicroBeads; *Miltenyi Biotec*, Germany) as described previously (Steiner et al., 2013). The MDM and MDDC were added on the apical ($5 \times 10^4$ cells/insert, *i.e.*, $1.19 \times 10^4$ cells/$cm^2$) and the basal ($25 \times 10^4$ cells/insert, *i.e.*, $5.59 \times 10^4$ cells/$cm^2$) side of the A549 layer, respectively. After a 24 h incubation under suspension conditions, in complete cell culture medium (cRPMI; *Sigma-Aldrich*, Switzerland; RPMI 1640 supplemented with 1 % L-Glutamine, 1 % Penicillin/Streptomycin and 10 % fetal bovine serum), the co-culture was transferred to the ALI (by extracting the cell medium from the apical layer and basolateral layer, and adding 1.2 mL of fresh cell medium on the basal side) for a period of 24 h prior to particle exposures. All cell cultures were maintained at the ALI (having the cRPMI only present on the basal side of the insert) throughout the exposure period (24 h).

### 2.3. Cell culture exposures

The multicellular lung model was separately exposed to respirable $SO_2$-exposed and control glass and pumice samples (Fig. 1) in order to deduce the response to either salt-laden particles or the particle substrate (control sample) alone. For direct deposition onto the cell cultures at the ALI, samples were nebulized in a dry state using a dry powder insufflator (Model DP-4; *PennCentury Inc.*, USA), as described previously (Tomašek et al., 2016, 2018).

Briefly, the sample was loaded into a sample chamber and then pushed through the insufflator by small pulses of air administered using a 10 mL commercial syringe. The ash was discharged as a cloud from the end of the delivery tube over the cell culture plate located within a closed nebulisation chamber. Placed next to the culture plate, a quartz crystal microbalance (QCM; *Stanford Research Systems,* USA) was used to monitor the cell-delivered dose of particles during the exposures. Deposited mass per area (μg/$cm^2$) was calculated based on the recorded frequency values after Lenz et al. (2009).

Whilst testing aerosolization of the samples, using the approach where equivalent sample feed masses were loaded into the dry powder insufflator (as done in our previous study (Tomašek et al., 2016)), it became apparent that achieving an equivalent mass exposure and reproducibility for different samples was challenging. The variations in deposition arose mainly due to the handling of the equipment which is also influenced by the nature of the chosen particles (*e.g.*, the internal surfaces of the device may be coated with powder, hence influencing the powder discharge). To overcome these issues, an approach was applied where deposition was monitored during the exposures (using the QCM) and the ash was nebulized until a targeted dose between 0.5 and 0.7 μg/$cm^2$ was reached, regardless of the feed mass. This mass-dose range was adopted from our previous study; however, we note that it likely deviates from a real-life exposure and represents a high concentration scenario (Tomašek et al., 2016).

### 2.4. Cellular assays and analysis

#### 2.4.1. Cell morphology

To assess potential changes to the cell cultures, *i.e.*, alteration of cellular morphology following exposure, in comparison to the untreated cells, samples were visualised by LSM. Cell cultures were prepared for imaging such that, during collection, cell membranes were fixed with 4 % paraformaldehyde for 15 min at room temperature, and then washed and stored in phosphate buffered saline (PBS). Subsequently, they were permeabilised with 0.2 % Triton X-100 + 1 % bovine serum albumin (BSA) in PBS for 15–30 min at room temperature. Following the permeabilisation step, samples were blocked with BSA to negate any non-specific binding of the primary antibody with the cell system. Samples were then stained with Phalloidin-Rhodamine (Molecular Probes, *Thermo Fisher Scientific Inc.*, USA) to label the F-actin cytoskeleton and 4',6-diamidin-2-phenylindole (DAPI; *Sigma-Aldrich*, Germany) to highlight the cell nuclei, diluted to 1:50 and 1:100 in 0.1 % BSA in PBS for 1–2 h at room temperature, respectively. Then they were mounted with a mounting medium Glycergel (*DAKO Schweiz AG*, Switzerland) on microscope slides. Visualisation of the samples was conducted with an inverted confocal LSM Zeiss 710 (*Carl Zeiss*, Switzerland) using a 63x/1.4 NA oil immersion lens. Representative images (z-stacks) were recorded and were further processed using the 3D reconstruction software IMARIS (*Bitplane AG*, Switzerland).

#### 2.4.2. Cytotoxicity

The level of cytotoxicity, *i.e.*, the potential of particles to cause cell membrane damage, was determined by measuring the release of the intracellular enzyme LDH into the co-culture supernatant using the LDH Cytotoxicity Detection Kit (*Roche Applied Science,* Germany) according to the manufacturer's protocol. The absorbance was determined at 490 nm using a microplate reader (*Bio-Rad,* Switzerland), with a reference wavelength set at 630 nm. As a positive control, co-cultures were treated with 100 μL of 0.2 % Triton X-100 in $H_2O$ applied on the apical side and incubated for 24 h (at 37 °C, 5 % $CO_2$). Triton X-100 induces cell lysis *(i.e.*, breaking down of the membrane) thus resulting in release of LDH into the supernatant. The negative control was the supernatant of the untreated cell culture.

#### 2.4.3. (Pro-)inflammatory cytokine release

In this study, the (pro-)inflammatory response was investigated by quantifying tumour necrosis factor alpha (TNF-α), interleukin 8 (IL-8) and interleukin 1β (IL-1β) release from the co-cultures by enzyme-linked immunosorbent assays (ELISA DuoSet Development Kit, *R&D Systems*, USA) according to the manufacturer's protocol. Analyses were conducted in triplicate for each biological repetition. The concentrations were determined spectrophotometrically at 450 nm using a microplate reader (*Bio-Rad,* Switzerland). Lipopolysaccharide (LPS, from *E. coli* at 1 μg/mL in cRPMI) applied as 1.2 mL solution in the bottom compartment of the cell co-cultures served as the positive control due to its known ability to promote the secretion of (pro-)inflammatory cytokines in the treated cells. The negative control was the supernatant of the untreated cell culture.

#### 2.4.4. Gene expression analysis

In the present study, we have assessed the expression levels of genes caspase 7 (*CASP7*) and FAS receptor (*FAS*) to observe the induction of cell death, heme oxygenase 1 (*HMOX1*) and NAD(P)H dehydrogenase [quinone] 1 (*NQO1*) to assess oxidative stress, and interleukin 1 beta (*IL1B)* and interleukin 8 (*IL8*) to determine (pro-)inflammatory responses. Quantification of gene expression was performed by Real-Time Quantitative Reverse Transcription Polymerase Chain Reaction (real-time qRT-PCR), as previously described (Rothen-Rutishauser et al., 2005). Cell cultures grown on membranes, collected following particle exposures, were stored in ribonucleic acid (RNA) protect buffer (RNAprotect® Cell Reagent; *Qiagen,* Germany) for up to 72 h and prior to the analysis. RNA was isolated with RNeasy® Plus kit (*Qiagen,* Germany). RNA concentrations in samples were analysed with a NanoDrop 2000 spectrophotometer (*Thermo Scientific*, USA). Complementary deoxyribonucleic acid (cDNA) synthesis was performed using the Omniscript® RT kit (*Qiagen*, Germany) according to the manufacturer's protocol. A real-time PCR was performed using SYBR® Green (*Applied Biosystems*,

USA) on a 7500 Fast Real-Time PCR system (*Applied Biosystems*, USA). Relative expression levels were calculated using the $2^{-\Delta\Delta Ct}$ method, with glyceraldehyde-3-phosphate dehydrogenase (*GAPDH*) as the standard gene.

#### 2.4.5. Ash-cell interactions

Exposed co-culture membranes were fixed with 4 % PFA (15 min, room temperature) and then sequentially washed with 20, 40 and 60 % methanol for 5 min, 80 % methanol for 3 min and washed 5 times with 100 % methanol for 30 s. Samples were then dried in a vacuum desiccator over a 48 h period. Samples were then carbon coated to a thickness of ~4 nm and subsequently imaged with a Mira 3 LM FE-SEM (*Tescan*, Czech Republic), using an InBeam detector on a rotated stage (60°). Operating parameters are noted in the figure caption.

### 2.5. Data and statistical analysis

All data are presented as the mean ± standard error of the mean derived from three individual experiments (n = 3), unless otherwise stated. Statistical significance was deduced through the use of a one-way analysis of variance (ANOVA), assuming normal distribution of all datasets. Subsequent Tukey's *post hoc* tests were conducted to determine the specific statistical significance between different exposures to the negative control. The alpha value was set at 0.05. All statistical analyses were performed using the software Origin (version 9.3, *OriginLab Corporation,* USA).

## 3. Results

### 3.1. Physical characterisation of particles

Results of the particle size analysis of isolated respirable fractions are reported in Table 1 and Fig. 2. Across different samples, particle size was largely comparable; *ca.* 90 % or greater by volume of particles were sub-10 μm diameter.

The generated particles were shown to be representative analogue materials for volcanic ash with regards to their shape, as observed by SEM (Fig. 3). Similar to the morphology generally observed for respirable volcanic ash (*e.g.*, Damby et al., 2016, Lahde et al., 2013, Horwell et al., 2013, Hillman et al., 2012, Le Blond et al., 2010), the particles were mostly blocky and angular with varying amounts of sub-micron particles adhering to the surfaces of larger particles (Figs. 3 and 4). The SEM analysis of generated ash particles also revealed an abundance of discrete salt deposits in the form of sub-micron sized nodules across the particle surfaces (Fig. 4).

### 3.2. Solubility of surface salts

The presence and the composition of the surface salt deposits on the $SO_2$-exposed samples are indicated by the leachate data (60 min time-point), where the dominant species in the water leachate solutions were $Ca^{2+}$, $Na^{+}$, $Mg^{2+}$ and $SO_4^{2-}$ (Table 2). These results indicate the presence of surface sulphate salt deposits on the ash particles, with the predominant species being $CaSO_4$ (Fig. 5). Charge balance calculations show that the major cations account for all of the $SO_4^{2-}$. The time-series leaching experiment showed that dissolution of surface deposits is relatively rapid, with the majority (approximately 90 % or greater for all elements and samples) of available soluble species being released from the particle surface within the first 10 min of leaching (Fig. 6).

PHREEQC modelling of the water leach data for the $SO_2$-exposed glass (G_$SO_2$) sample showed that, at the three experimental times (10, 30 and 60 min), the solutions were undersaturated (at 25 °C, pH 7.4) with respect to $CaSO_4$ (anhydride), with SI values ranging from −2.53 (10 min) to −2.43 (60 min). These results indicate that $CaSO_4$ on the sample surface would dissolve and that the water leachate solutions have the potential to further dissolve $CaSO_4$. Given that the release of Ca and $SO_4$ decreased considerably after 10 min (as seen in Fig. 6), most of the $CaSO_4$ surface salt deposits on the ash particles had probably dissolved after 60 min. A similar potential to dissolve $CaSO_4$ was observed for PHREEQC modelling with SLF. The SLF solution itself is undersaturated with respect to $CaSO_4$, with a calculated SI of −6.97. When the same amounts of Ca, Na, Mg and $SO_4$ measured in the water leaching experiments (Fig. 6) are added to the model SLF solution (this assumes that an equivalent abundance of surface deposits will dissolve in SLF as seen in the water leaching experiments, which is reasonable given the initial saturation value), PHREEQC simulations indicate that the final solutions would still be highly undersaturated with respect to $CaSO_4$, with a final SI of −5.66.

### 3.3. Nebulisation of analogue particles

The averages of cell-deposited doses of nebulized particles ranged between 0.48 and 0.69 μg/cm$^2$ (Fig. 7). The glass samples (G_$SO_2$ and G_CTRL) were deposited within a tighter range in comparison to the pumice samples.

### 3.4. Ash particle toxicity

For the assessed biological endpoints (cytotoxicity, oxidative stress and (pro-)inflammatory mediators, including measurements for both protein production and gene expression), no significant ($p > 0.05$) changes were observed following cell culture exposures to any of the particle types after 24 h, for the dose range tested.

Images acquired by LSM showed no changes in cell morphology when compared to the negative control (untreated cells; Fig. 8A). The release of LDH by the cells did not differ significantly ($p > 0.05$) from the negative control for different particle type treatments, while it was significantly ($p < 0.05$) increased for the positive assay control Triton X-100, confirming the responsiveness of the biological model used for the measured endpoint (Fig. 8B). Regarding the expression of (pro-) apoptotic genes *FAS* and *CASP7*, none of the exposures showed a statistically significant ($p > 0.05$) outcome (Fig. 8C). In addition, there was no statistical difference in gene expression between different particle types.

The expression of *HMOX1* and *NQO1*, genes related to oxidative stress, showed no significant ($p > 0.05$) increase of gene expression levels after particle exposures when compared to the negative control (Fig. 9).

No significant ($p > 0.05$) (pro-)inflammatory response was observed for any particle, as measured for the chosen markers. Increased production of IL-8 compared to the negative control samples was observed after exposure to all the particles, however, the levels did not differ significantly from those in the negative control sample (Fig. 10A), whereas the levels of TNF-α and IL-1β were below the method detection limits (data not shown). In agreement with the protein measurements, none of the cell treatments induced a change in the mRNA levels of (pro-)inflammatory markers measured relative to those in the negative control sample (Fig. 10B).

**Table 1**
Particle size information at health-relevant size fractions for the isolated respirable samples of $SO_2$-exposed glass (G_$SO_2$) and pumice (P_$SO_2$) and their respective controls (G_CTRL and P_CTRL). Data are the mean of n = 3.

| Sample | Particle size (cum. vol. %) | | | |
|---|---|---|---|---|
| | < 1 μm | < 2.5 μm | < 4 μm | < 10 μm |
| G_$SO_2$ | 13.2 | 25.9 | 45.2 | 95.6 |
| G_CTRL | 10.8 | 26.6 | 47.3 | 97.7 |
| P_$SO_2$ | 7.0 | 22.8 | 43.7 | 90.0 |
| P_CTRL | 5.9 | 23.4 | 44.1 | 88.6 |

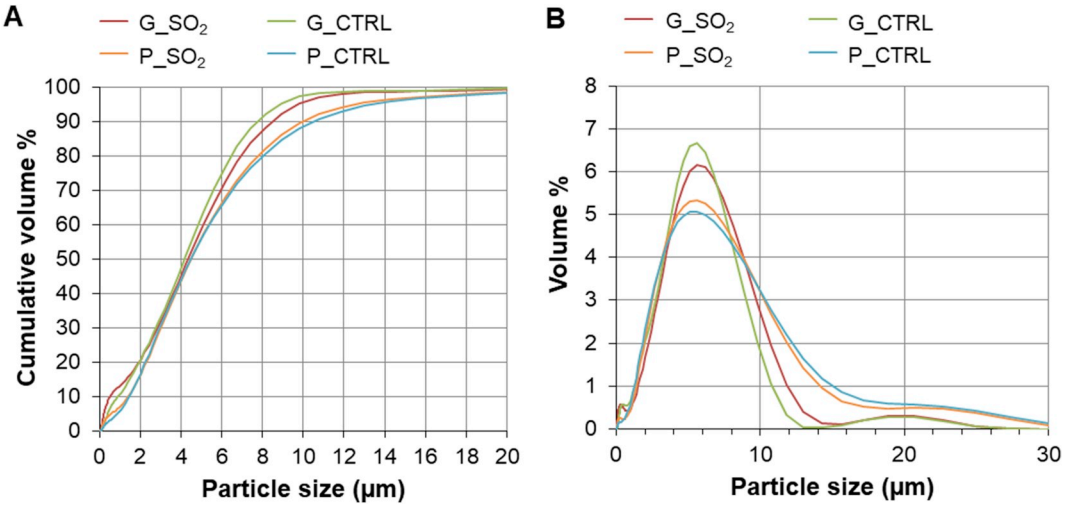


**Fig. 2. Particle sizing data of respirable post-AGAR samples. A)** Cumulative particle size distributions and **B)** particle size distributions of samples. Three measurement cycles were recorded for each sample ($SO_2$-exposed glass (G_$SO_2$) and pumice (P_$SO_2$) and their respective controls (G_CTRL and P_CTRL)) and an average taken.

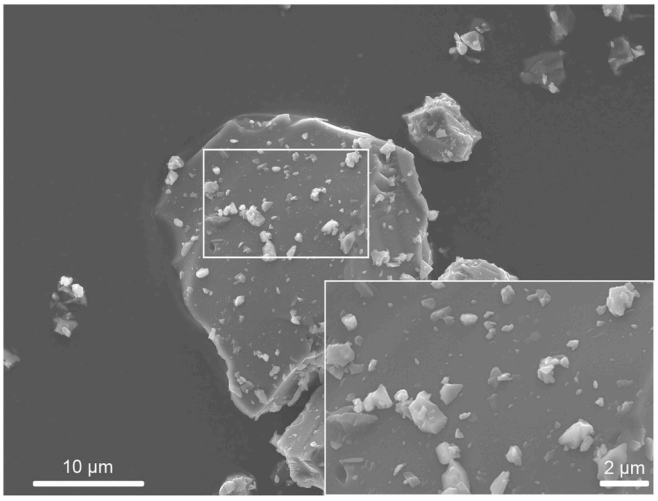


**Fig. 3. Representative scanning electron micrographs of synthetic volcanic glass particles exposed to Ar gas (G_CTRL) for 2 h at 500 °C in the AGAR.** Images were collected at 10.0 kV and 8.1 mm working distance. Scale bars are noted on the images.

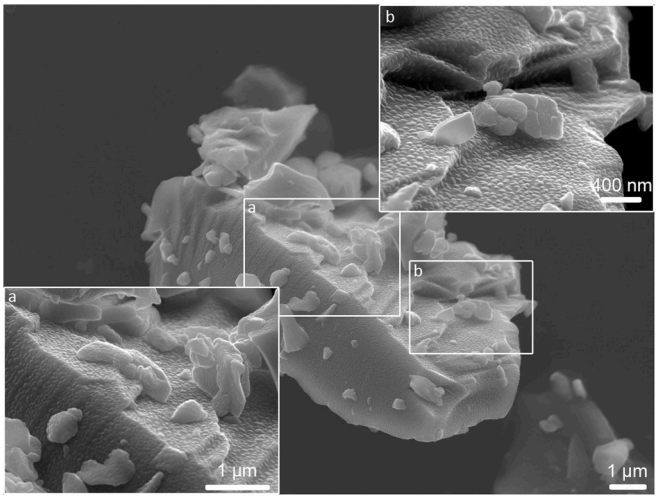


**Fig. 4. Representative scanning electron micrographs of $SO_2$-exposed synthetic volcanic glass particles (G_$SO_2$), exposed to $SO_2$ gas for 2 h at 500 °C in the AGAR.** The result of interaction is formation of sulphate salts on the particle surface, in the form of nanometre-scale surface nodules, as shown in insets **a)** and **b)**. Images were collected at 10.0 kV and 9.1 mm working distance. Scale bars are noted on the images.

## 4. Discussion

This study is the first to investigate the potential for in-plume $SO_2$ gas-ash interactions to influence volcanic ash reactivity *in vitro*. The results show that surface salt deposits on the $SO_2$-exposed samples leach into water (or SLF) relatively rapidly, with the majority of available soluble species leaching from the particle surface within the first 10 min of the experiment. Exposure of the multicellular human lung model to artificially generated pristine and $SO_2$-exposed volcanic particulate did not induce significant effects on any of the biological endpoints measured (cytotoxicity, oxidative stress and (pro-)inflammatory response). This indicates that the surface salt deposits, and the underlying alterations to the substrate resulting from particle processing in the AGAR, do not cause acute adverse effects either *via* particle uptake or through reactions of cells with the salt-enriched cell lining fluid.

### 4.1. In-plume processing of volcanic ash

The concentrations of $SO_4^{2-}$ in sample leachate solutions were measured in volcanically relevant quantities: up to 2008 ± 13 mg/kg compared to a mean concentration of 2172 mg/kg from a global dataset (see Ayris and Delmelle (2012) and Table 2). Accordingly, the outcomes of this study have directrelevance to natural volcanic ash exposures.

**Table 2**
Mean concentration ( ± standard error of the mean) of water-extractable major elements from the samples used in the present study (determined after leaching for 60 min; n = 3) and from the global dataset (the data are from 27 to 30 discrete studies) (Ayris and Delmelle, 2012)*. Here, sulphate is expressed as S for convenience in the comparison with the reported mean concentrations in the global dataset. Data are reported as milligram of element per kilogram of ash (mg/kg).

| | Ca | S | Na | Mg |
|---|---|---|---|---|
| G_$SO_2$ | 2008 ± 13 | 1893 ± 12 | 242 ± 6 | 217 ± 3 |
| G_CTRL | 155 ± 1 | 3 ± 0.3 | 78 ± 1 | 72 ± 1 |
| P_$SO_2$ | 710 ± 20 | 806 ± 8 | 236 ± 16 | 128 ± 2 |
| P_CTRL | 249 ± 2 | 120 ± 2 | 132 ± 0.4 | 58 ± 1 |
| Global dataset* | 2172 | 1711 | 407 | 349 |

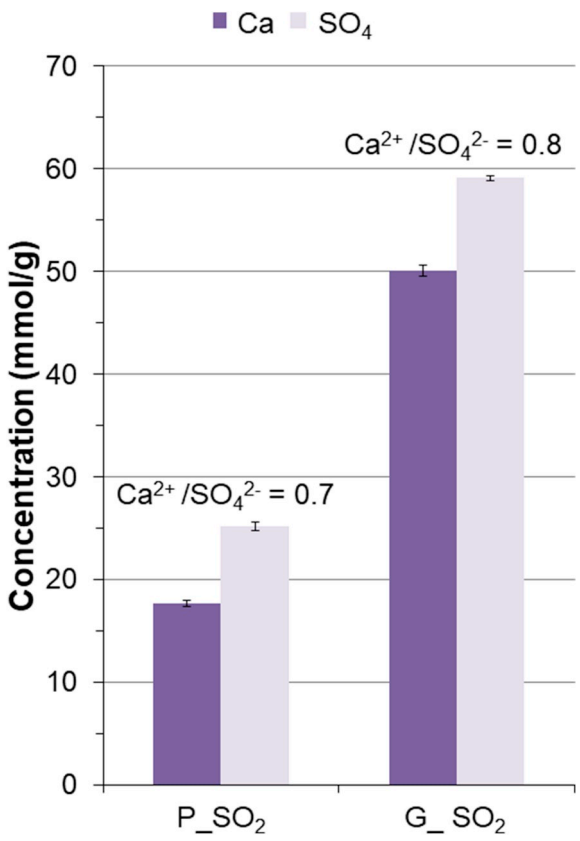


**Fig. 5. Ratio of $Ca^{2+}$ to $SO_4^{2-}$ abundance (mmol/g) in $SO_2$-exposed pumice (P_$SO_2$) and glass (G_$SO_2$)** measured in solutions extracted after 60 min leaching in deionized water. The data are shown as the mean ± standard error of the mean (n = 3).

Measured concentrations of $Ca^{2+}$ and $SO_4^{2-}$ indicated that the dominant reaction product following exposures in the AGAR was likely $CaSO_4$. This is in congruence with earlier experiments investigating scavenging of $SO_2$ by silicate glass particles of varying compositions (Ayris et al., 2013; Delmelle et al., 2018). The presence of these elements on the ash surface, as $CaSO_4$ salt, is usually confirmed from stoichiometric calculations of $Ca^{2+}$ to $SO_4^{2-}$ ratios in water leachate, which should be approximately 1:1 (Rose et al., 1973; Rose, 1977; De Hoog et al., 2001). Here, the $Ca^{2+}$ to $SO_4^{2-}$ ratios were 0.7 and 0.8 for $SO_2$-exposed glass and pumice (Fig. 5), respectively, indicating that, in addition to $CaSO_4$, different sulphate salts must also have formed. Since $Na^+$ and $Mg^{2+}$ were also measured in the leachates, it is clear that the particles contained Na- and Mg-bearing soluble phases, concentrations of which increased following the $SO_2$ exposure in the AGAR (Table 2). These are likely to be $Na_2SO_4$ and $MgSO_4$ surface deposits, although they have only been inferred to exist on volcanic ash in previous leachate studies (Olsson et al., 2013; Bagnato et al., 2013; De Hoog et al., 2001; Rose, 1977). The presence of $Na_2SO_4$ on our samples is further supported by previous reaction-temperature experiments on experimental glass powders, which show that $Na_2SO_4$ can co-exist with $CaSO_4$ at 300–600 °C (Ayris et al., 2013).

Following experiments in the AGAR, and in agreement with previous studies (Maters et al., 2016, 2017), simulated volcanic glass was shown to be more reactive towards $SO_2$ than pumice. This is evident from the concentration of $SO_4^{2-}$ in the water leachate data (Fig. 6), which results from the higher abundance of soluble S-bearing products on the glass surface resulting from the gas uptake. This could be attributed to the differences in diffusion rate of $Ca^{2+}$ from the particle interior to the surface (Ayris et al., 2013), which is supported by the observation of a lower concentration of $Ca^{2+}$ in the pumice water leachate (Fig. 6).

Whilst, in the present experiments, $Ca^{2+}$, $Na^+$, $Mg^{2+}$ and $SO_4^{2-}$ are the most abundant soluble species available to interact with the lung model, it has to be taken into account that natural volcanic ash will exhibit variabilities in the nature and abundance of surface salts (Olsson et al., 2013; Ayris and Delmelle, 2012; Witham et al., 2005). For example, ash generated through disruption of a hydrothermal system (*e.g.*, in a phreatic explosion) is likely to be much higher in salt deposits than ash generated from fragmented magma, as the interaction of the lithic material (the volcanic edifice) with hydrothermal fluids may increase concentrations of certain elements (Witham et al., 2005). In the plume, volcanic HCl gas is also being scavenged by particle surfaces, forming Cl-bearing salts such as NaCl, $CaCl_2$ and $MgCl_2$ (Witham et al., 2005; Ayris and Delmelle, 2012; Ayris et al., 2014). Since HCl gas was not used during the AGAR experiments, the post-AGAR samples lacked such typical salt deposits. This was confirmed by the low release of soluble chloride in the water leach (data not shown) and with the absence of identifiable NaCl cubic structures by SEM imaging (Fig. 4) (Ayris et al., 2014). Thus, any biological responses elicited in the *in vitro* human lung system exposed to glass and pumice in the current study are discussed with regards to the presence of sulphate salts only.

### 4.2. The effects of interactions with $SO_2$ gas on ash toxicity in vitro

To get an insight into the likely mechanism underlying the cellular responses following ash particle exposures, it was necessary to understand whether the salts would interact with cells while still on the ash particle surface, or whether they would dissolve upon contact with the liquid lining layer of the multicellular model, prior to particle uptake. Endocytosis, *i.e.*, the uptake of substances by some cell types, such as macrophages and epithelial cells, is a relatively rapid process where particles may be engulfed within 10 min of making contact with the cell (Paul et al., 2013). This means that particles deposited in the vicinity of a macrophage could have been taken up within the first 10 min following exposure, but it is likely that others were engulfed at a later point during the experiment since macrophages do not cover the entire surface of the lung epithelium (Pinkerton et al., 2015). Therefore, 10 min was considered the minimum duration for particles to interact with lung fluid. The dissolution rate experiments showed that the majority of soluble $CaSO_4$ deposits are dissolved from the particle surface after only 10 min contact time with deionized water (Fig. 6). Reaction-path modelling with PHREEQC showed that the SLF solution is undersaturated with respect to sulphate salts, suggesting that salt deposits would also dissolve in lung fluid. Therefore, it is likely that the dissolution of salt deposits occurred prior to particle uptake, at least in part, with soluble compounds being dispersed and diluted in the cell lining fluid.

The major cations present in our ash leachates ($Ca^{2+}$, $Na^+$ and $Mg^{2+}$) are physiologically important ions required for normal function of cells. Their intra- and extracellular concentrations are optimally maintained in a dynamic state of equilibrium, *i.e.*, they are able to cross cell membranes if required by the cells, in order to maintain tissue homeostasis (Yang and Hinner, 2015). In turn, the excess of such ions may alter cell homeostasis and activate various complex signalling pathways (*e.g.*, calcium signalling) and, in this way, potentially induce toxicity (*e.g.*, Brown et al., 2004, Donaldson et al., 2003, Schorn et al., 2011). For example, a study by Könczöl et al., 2012 found that $CaSO_4$ particles (applied as a suspension in cell medium and, thus, dissolved to a considerable extent) were able to mediate reactive oxygen species (ROS) generation and induce DNA damage in A549 cells *in vitro*, but at doses as high as 100 $\mu g/cm^2$. In comparison, *in vitro* studies on V79 cells (Chinese hamster lung cells) or IMR90 cells (human lung fibroblasts) have used $CaSO_4$ as a negative particle control and did not observe any toxic effects for doses $< 20\ \mu g/cm^2$ (Dopp et al., 2005; Geh et al., 2006). When compared to these studies, the amount of $CaSO_4$ dissolved from glass ($3.95 \times 10^{-3}\ \mu g/cm^2$) and pumice ($1.39 \times 10^{-3}\ \mu g/cm^2$)

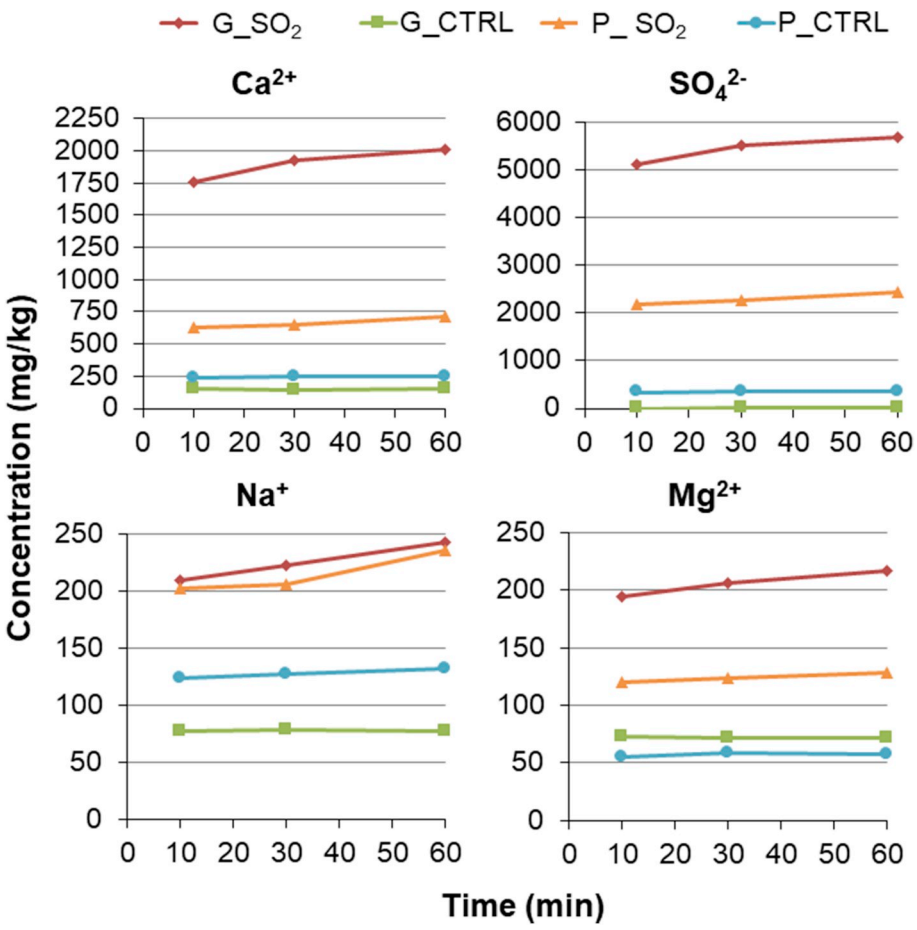


**Fig. 6. Plot of major element concentration of $SO_2$-exposed glass (G_$SO_2$) and pumice (P_$SO_2$) and their respective controls (G_CTRL and P_CTRL)** measured in solutions extracted after 10, 30 and 60 min leaching in deionized water. The data shown are from the following repetitions: 10 min n = 1, 30 min n = 1 and 60 min the average of n = 3. Data are reported as milligram of element per kilogram of ash (mg/kg).

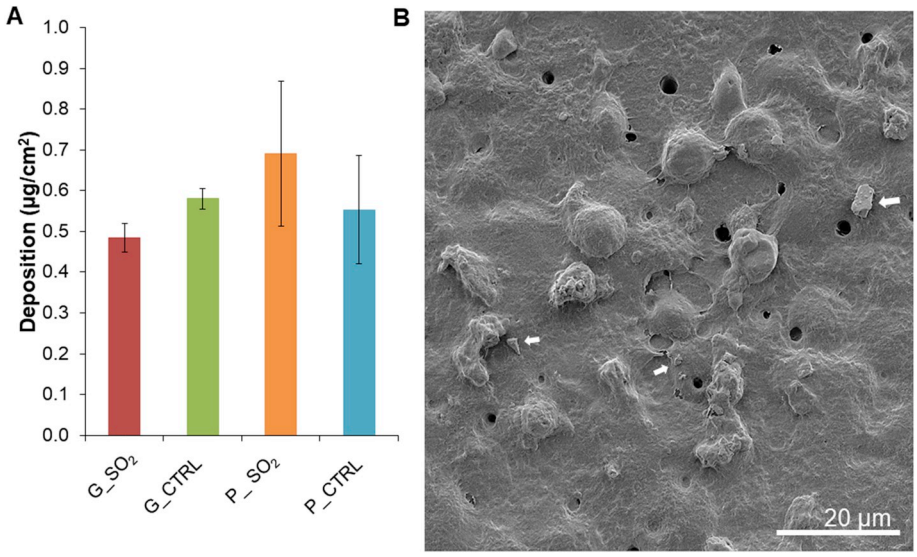


**Fig. 7.** Deposition of nebulized respirable fraction of $SO_2$-exposed and control glass and pumice samples. A) Average mass deposition (µg/cm$^2$) of $SO_2$-exposed glass (G_$SO_2$) and pumice (P_$SO_2$) and their respective controls (G_CTRL and P_CTRL) quantified using a quartz crystal microbalance (QCM), following their dry nebulisation using a dry powder insufflator (DP-4, *Penn Century*, USA). Data are shown as the mean ± standard error of the mean, related to the following repetitions for each exposure: G_$SO_2$ and G_CTRL n = 5, P_$SO_2$ and P_CTRL n = 3. **B)** Representative scanning electron micrograph of the apical side of the multicellular lung model, showing deposited particles (indicated with white arrows). The image was collected at 2 kV and 16.13 mm working distance. Scale bar is 20 µm.

particles in the present study is negligible. Damby et al. (2018)argued a similar negligible impact for $Na^+$ concentrations equivalent to those measured in the present study. Concentration of $Mg^{2+}$ is also tightly regulated by cells, whereby changes might influence cellular function (Romani and Scarpa, 2000; Romani, 2011). Given that intra- and extracellular concentrations of free $Mg^{2+}$ are on the order 10 mmoL/L and 1 mmoL/L, respectively, and an average experimental ash dose of 0.5 µg/cm$^2$ introduces less than 10 nmoL $Mg^{2+}$, it is reasoned that, as with $Ca^{2+}$, $Na^+$ and $SO_4^{2}$, the slight increase in the already heavily buffered cell lining fluid following ash exposures would have an insignificant impact on the chemistry of the solution and, consequently, cellular function.

The response to $SO_2$-exposed and control glass and pumice samples was negligible, overall, and comparable across all measured biological endpoints which, contrary to the hypothesis, indicates that the presence of salt deposits does not affect the biological reactivity of volcanic ash. The lack of significant impact on cell viability, as measured by the release of LDH and the expression of (pro-)apoptotic genes *FAS* and

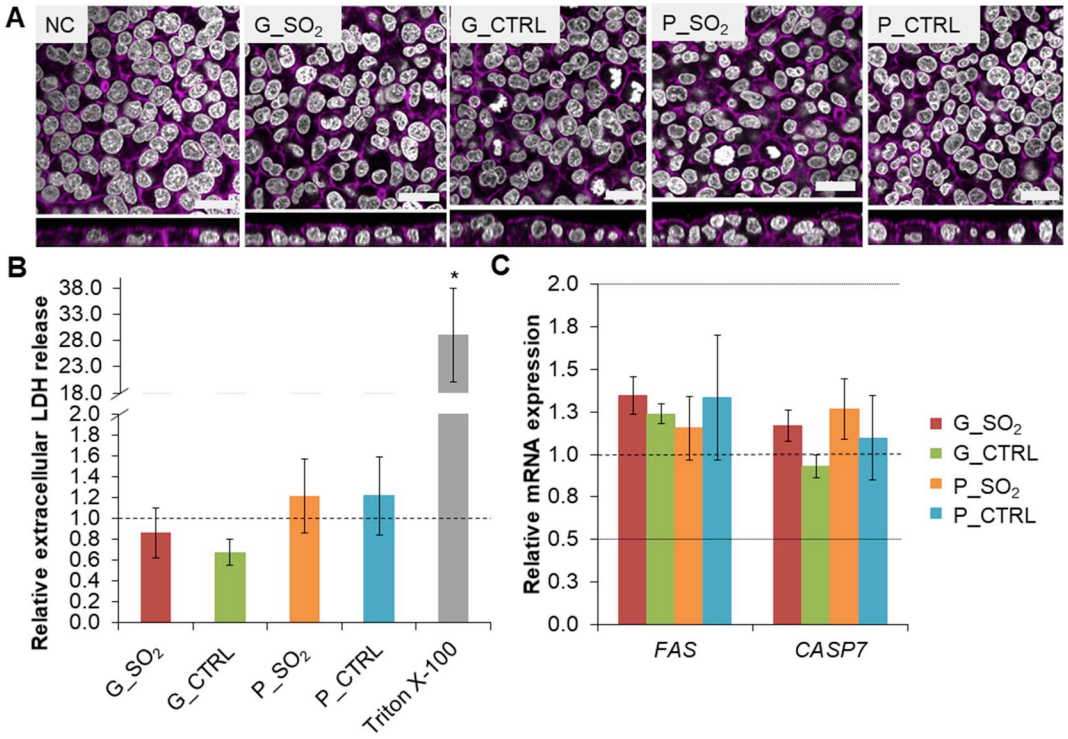


**Fig. 8. Cell morphology and cell viability of the multicellular lung model following exposures to $SO_2$-exposed glass and pumice particles. A)** Representative LSM images from XY and XZ projections for cell cultures exposed to $SO_2$-exposed glass (G_$SO_2$) and pumice (P_$SO_2$) and their respective controls (G_CTRL and P_CTRL), including the negative control (NC; untreated cells). Cells were stained with Phalloidin-Rhodamine (F-actin cytoskeleton, magenta) and DAPI (cell nuclei, grey). Scale bars are 20 μm. **B)** Extracellular LDH levels in the culture medium normalized to the negative control (supernatant of the untreated cells). The positive assay control was supernatant from the cells exposed apically to 0.2 % Triton X-100 in PBS for 24 h. Data are presented as the mean ± standard error of the mean. The data shown are from the following repetitions for each exposure: G_$SO_2$ and G_CTRL n = 5, P_$SO_2$ and P_CTRL n = 3. * denotes significant difference ($p < 0.05$) between positive control and the other samples tested. **C)** Relative amounts of mRNA of (pro-)apoptotic genes FAS receptor (*FAS*) and caspase 7 (*CASP7*). Data are presented as the mean ± standard error of the mean, related to the following repetitions for each exposure: G_$SO_2$ n = 5, G_CTRL n = 4, P_$SO_2$ and P_CTRL n = 3. The two horizontal lines represent a one-half decrease (0.5) and a two-fold increase (2.0) in the mRNA content of the specific gene, relative to its content in untreated cells and the housekeeping gene (*GAPDH*) in the same sample (1.0, dashed line).

*CASP7*, and low oxidative stress potential of all particles, is in agreement with previous research investigating ash toxicity *in vitro* (Cullen and Searl, 1998; Wilson et al., 2000; Damby et al., 2013, 2016; Horwell et al., 2013; Tomašek et al., 2018), despite the different substrates and application of salt deposits. The minimal (pro-)inflammatory response observed for all particle treatments is largely in congruence with the aforementioned *in vitro* studies. Yet, the results suggest that volcanic glass has a potential to initiate an inflammatory response. While non-significant, exposure to $SO_2$-exposed glass (G_$SO_2$) resulted in a slight increase in IL-8 production by the cells compared to the negative control, at both protein secretion and gene levels (Fig. 10). Such response could be a consequence of changes in oxidative stress status, indicated by a non-significant upregulation of *HMOX1* (an oxidative stress-related gene; Fig. 9), as inflammation may be resultant of, but not confined to, increased production of oxidants by macrophages in response to the insult posed by particles and upon ingestion of particles. In addition, exposure to the glass control sample (G_CTRL) caused relatively high, but non-significant, expression of both *IL8* and *IL1B* compared to the negative control and other particle treatments (Fig. 10B). Although this is difficult to state due to the lack of significant effects observed, these observations suggest that the glass (substrate) itself may be involved in the immune response to volcanic particulate (Ghiazza et al., 2010; Damby et al., 2018). This further implies that the underlying alterations that resulted from particle interactions with $SO_2$ and processing in the AGAR did not affect substrate biological reactivity in the current experimental conditions.

## 5. Conclusion

This study provides the first insight into the potential for reactions that occur within an eruptive plume to affect the biological reactivity of volcanic ash. This was accomplished by replicating in-plume reactions in a laboratory setting and measuring changes in the biological effects of volcanic ash exposures *in vitro*.

The presence of soluble sulphate compounds on the particle surface has no adverse biological impact to a multicellular human lung model in an acute exposure scenario, with the biological endpoints measured. We show that emplaced surface salts are likely to dissolve in the lungs prior to the cellular uptake, and any changes in ash surface chemical functionalities associated with the experimental ash-$SO_2$ reactions do not impact ash toxicity. The presence of substantial amounts, but still in the physiological range, of $Ca^{2+}$, $Na^{+}$, $Mg^{2+}$ and $SO_4{}^{2-}$ in ash-water leachates also does not correspond with a change in ash toxicity. These results suggest that interaction of volcanic ash with $SO_2$ during ash generation and transport does not significantly affect the respiratory toxicity of volcanic ash. Therefore, sulphate salts are unlikely to be a dominant factor controlling variability in *in vitro* toxicity assessments observed during previous eruption response efforts.

The observations of this study advance the understanding of the overall hazard posed by volcanic ash through consideration of aspects of in-plume processing on ash toxicity, thus providing valuable information for health risk assessment in future volcanic eruption events. However, volcanic plumes comprise many species, including halogens and trace metals, that may alter the ash surface or negatively impact

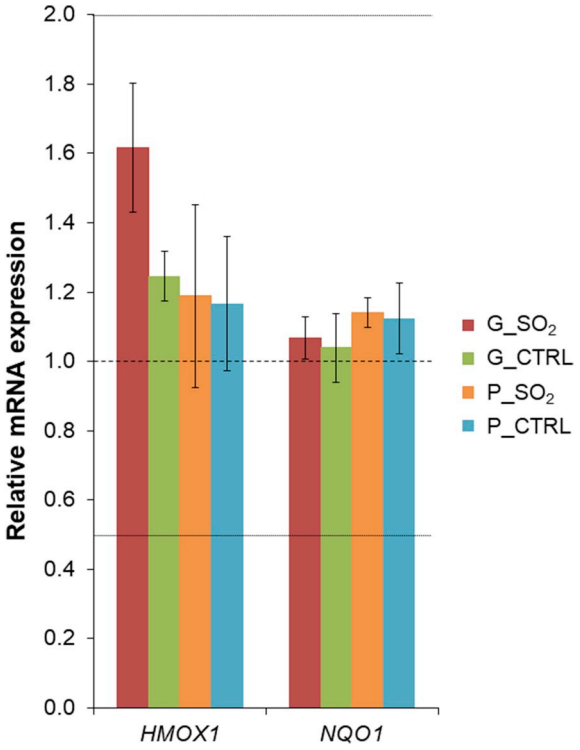


**Fig. 9. Oxidative stress response in the multicellular lung model following exposure to $SO_2$-exposed glass and pumice particles.** Relative amounts of mRNA for oxidative stress responsive genes, heme oxygenase 1 (*HMOX1*) and NAD(P)H dehydrogenase [quinone] 1 (*NQO1*). Data are presented as the mean ± standard error of the mean. The data shown are from the following repetitions for each exposure: G_$SO_2$ n = 5, G_CTRL n = 4, P_$SO_2$ and P_CTRL n = 3. The two horizontal lines represent a one-half decrease (0.5) and a two-fold increase (2.0) in the mRNA content of the specific gene, relative to its content in untreated cells and the housekeeping gene (*GAPDH*) in the same sample (1.0, dashed line).

health directly. Therefore, further investigations into the impact of in-plume processing of volcanic ash on pulmonary responses are warranted and should consider the importance of different particle compositions and volcanic gases, including associated changes to surface chemical functionalities and whether they can be correlated with biological responses *in vitro*.


## Funding information

This work was supported by the Marie Skłodowska-Curie Initial Training Network 'VERTIGO', funded through the European Seventh Framework Program (FP7 2007–2013) under grant agreement number 607905. We acknowledge the support of the University of Fribourg Scholarship (granted to IT in 2016/2017) and the Adolphe Merkle Foundation. IT acknowledges the support by the VUB Strategic Research Program (SRP) during the manuscript preparation. DED, PMA and DBD acknowledge the ERC Advanced Grant—Explosive Volcanism in the Earth System: Experimental Insights (EVOKES, no. 247076) awarded to DBD.


## Ethics approval and consent to participate

Not applicable.

## Consent for publication

All authors have read and approved the manuscript for publication.

## Availability of data and material

The datasets used and/or analysed during the current study are available from the corresponding author on reasonable request.

## Declaration of competing interest

The authors declare no conflict of interest. The authors are responsible for the content of the manuscript.


## Acknowledgements

Thanks to Jacopo Taddeucci, Piergiorgio Scarlato, Manuela Nazzari and Pierre-Yves Tournigand of HP-HT laboratory (National Institute of Geophysics and Volcanology (INGV) Roma, Italy) for their support in Rome. Thanks to Laetitia Haeni and Yuki Umehara for their assistance in the laboratory, as well as the BioNanomaterials group at the Adolphe


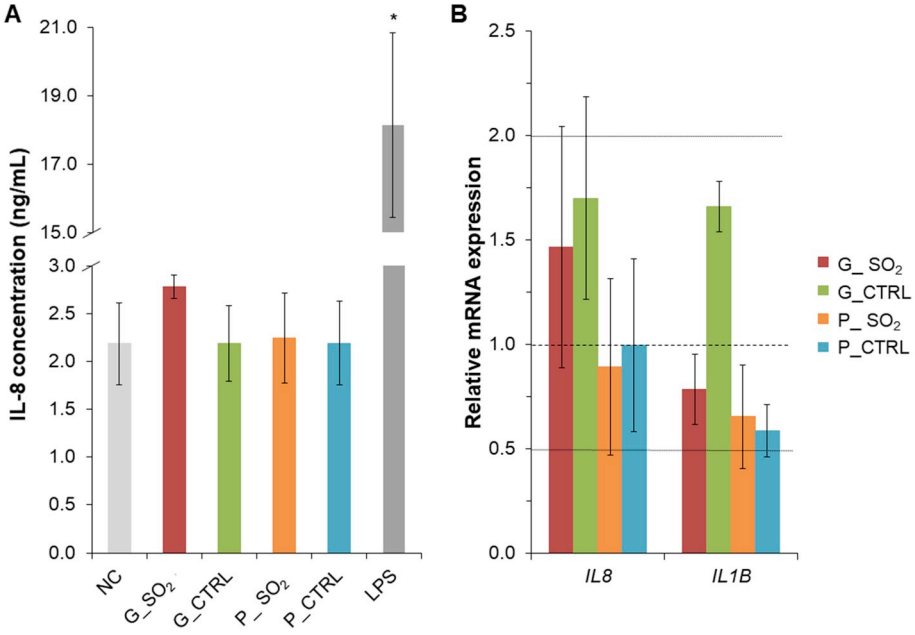


**Fig. 10. Release of (pro-)inflammatory mediators in the multicellular lung model following exposure to $SO_2$-exposed glass and pumice particles. A)** Interleukin-8 (IL-8) release in the culture medium following exposures to $SO_2$-exposed glass (G_$SO_2$) and pumice (P_$SO_2$) and their respective controls (G_CTRL and P_CTRL). The positive assay control was supernatant from the cells exposed to lipopolysaccharide (LPS; 1 μg/mL). The negative control (NC) was the supernatant of the untreated cells. Data are presented as the mean ± standard error of the mean (n = 3). * denotes significant difference ($p < 0.05$) between the positive control and the other samples tested. **B)** Relative amounts of mRNA of (pro-)inflammation-related genes encoding IL-8 (*IL8*) and IL-1β (*IL1B*). All data are presented as the mean ± standard error of the mean. The data shown are related to the following repetitions for each exposure: G_$SO_2$ n = 5; G_CTRL, P_$SO_2$ and P_CTRL n = 3. The two horizontal lines represent a one-half decrease (0.5) and a two-fold increase (2.0) in the mRNA content of the specific gene, relative to its content in untreated cells and the housekeeping gene (*GAPDH*) in the same sample (1.0, dashed line).

Merkle Institute. Thanks to Amanda Hayton and Kathryn Melvin (Department of Geography, Durham University, UK) for their help with IC analysis of ash leachates. We are thankful to Courtney Creamer and two anonymous reviewers for their constructive comments on this manuscript. Any use of trade, firm or product names is for descriptive purposes only and does not imply endorsement by the U.S. Government.

## References

Ayris, P.M., Delmelle, P., 2012. The immediate environmental effects of tephra emission. Bull. Volcanol. 74 (9), 1905–1936. https://doi.org/10.1007/s00445-012-0654-5.

Ayris, P.M., Lee, A.F., Wilson, K., Kueppers, U., Dingwell, D.B., Delmelle, P., 2013. SO2 sequestration in large volcanic eruptions: high-temperature scavenging by tephra. Geochem. Cosmochim. Acta 110, 58–69. https://doi.org/10.1016/j.gca.2013.02.018.

Ayris, P.M., Delmelle, P., Cimarelli, C., Maters, E.C., Suzuki, Y.J., Dingwell, D.B., 2014. HCl uptake by volcanic ash in the high temperature eruption plume: mechanistic insights. Geochem. Cosmochim. Acta 144, 188–201. https://doi.org/10.1016/j.gca.2014.08.028.

Ayris, P., Cimarelli, C., Delmelle, P., Wadsworth, F., Vasseur, J., Suzuki, Y., et al., 2015. A novel apparatus for the simulation of eruptive gas-rock interactions. Bull. Volcanol. 77 (12), 1–5. https://doi.org/10.1007/s00445-015-0990-3.

Bagnato, E., Aiuppa, A., Bertagnini, A., Bonadonna, C., Cioni, R., Pistolesi, M., et al., 2013. Scavenging of sulphur, halogens and trace metals by volcanic ash: the 2010 Eyjafjallajokull eruption. Geochem. Cosmochim. Acta 103, 138–160. https://doi.org/10.1016/j.gca.2012.10.048.

Barsotti, S., Andronico, D., Neri, A., Del Carlo, P., Baxter, P., Aspinall, W., et al., 2010. Quantitative assessment of volcanic ash hazards for health and infrastructure at Mt. Etna (Italy) by numerical simulation. J. Volcanol. Geotherm. Res. 192 (1), 85–96. https://doi.org/10.1016/j.jvolgeores.2010.02.011.

Baxter, P.J., 2000. Impacts of eruptions on human health. Encycl. Volcanoes 1035–1043.

Baxter, P.J., Ing, R., Falk, H., French, J., Stein, G.F., Bernstein, R.S., et al., 1981. Mount St Helens eruptions, May 18 to June 12, 1980: an overview of the acute health impact. JAMA 246 (22), 2585–2589.

Baxter, P.J., Ing, R., Falk, H., Plikaytis, B., 1983. Mount St. Helens eruptions: the acute respiratory effects of volcanic ash in a North American community. Arch. Environ. Health 38 (3), 138–143. https://doi.org/10.1080/00039896.1983.10543994.

Bérubé, K.A., Jones, T.P., Housley, D.G., Richards, R.J., 2004. The respiratory toxicity of airborne volcanic ash from the Soufrière Hills volcano, Montserrat. Mineral. Mag. 68 (1), 47–60. https://doi.org/10.1180/0026461046810170.

Blank, F., Rothen-Rutishauser, B., Gehr, P., 2007. Dendritic cells and macrophages form a transepithelial network against foreign particulate antigens. Am. J. Respir. Cell Mol. Biol. 36 (6), 669–677. https://doi.org/10.1165/rcmb.2006-0234OC.

Brown, D., Donaldson, K., Borm, P., Schins, R., Dehnhardt, M., Gilmour, P., et al., 2004. Calcium and ROS-mediated activation of transcription factors and TNF-α cytokine gene expression in macrophages exposed to ultrafine particles. Am. J. Physiol. Lung Cell Mol. Physiol. 286 (2), L344–L353. https://doi.org/10.1152/ajplung.00139.2003.

Buist, A.S., Vollmer, W.M., Johnson, L.R., Bernstein, R.S., McCamant, L.E., 1986. A four-year prospective study of the respiratory effects of volcanic ash from Mt. St. Helens 1–4. Am. Rev. Respir. Dis. 133 (4), 526–534. https://doi.org/10.1164/arrd.1986.133.4.526.

Carlsen, H.K., Gislason, T., Benediktsdottir, B., Kolbeinsson, T.B., Hauksdottir, A., Thorsteinsson, T., et al., 2012. A survey of early health effects of the Eyjafjallajökull 2010 eruption in Iceland: a population-based study. BMJ Open 2 (2), e000343. https://doi.org/10.1136/bmjopen-2011-000343.

Carter, J.D., Ghio, A.J., Samet, J.M., Devlin, R.B., 1997. Cytokine production by human airway epithelial cells after exposure to an air pollution particle is metal-dependent. Toxicol. Appl. Pharmacol. 146 (2), 180–188. https://doi.org/10.1006/taap.1997.8254.

Cho, W.-S., Duffin, R., Poland, C.A., Howie, S.E., MacNee, W., Bradley, M., et al., 2010. Metal oxide nanoparticles induce unique inflammatory footprints in the lung: important implications for nanoparticle testing. Environ. Health Perspect. 118 (12), 1699. https://doi.org/10.1289/ehp.1002201.

Cho, W.-S., Duffin, R., Poland, C.A., Duschl, A., Oostingh, G.J., MacNee, W., et al., 2012. Differential pro-inflammatory effects of metal oxide nanoparticles and their soluble ions in vitro and in vivo; zinc and copper nanoparticles, but not their ions, recruit eosinophils to the lungs. Nanotoxicology 6 (1), 22–35. https://doi.org/10.3109/17435390.2011.552810.

Cronin, S.J., Neall, V.E., Lecointre, J.A., Hedley, M.J., Loganathan, P., 2003. Environmental hazards of fluoride in volcanic ash: a case study from Ruapehu volcano, New Zealand. J. Volcanol. Geotherm. Res. 121 (3–4), 271–291. https://doi.org/10.1016/s0377-0273(02)00465-1.

Cullen, R.T., Searl, A., 1998. Preliminary toxicological hazard assessment of Montserrat volcanic ash: in vitro cytotoxicity. Institute of Occupational Medicine, Edinburgh, pp. 13 P752/200.

Damby, D.E., Horwell, C.J., Baxter, P.J., Delmelle, P., Donaldson, K., Dunster, C., et al., 2013. The respiratory health hazard of tephra from the 2010 Centennial eruption of Merapi with implications for occupational mining of deposits. J. Volcanol. Geotherm. Res. 261, 376–387. https://doi.org/10.1016/j.jvolgeores.2012.09.001.

Damby, D.E., Murphy, F.A., Horwell, C.J., Raftis, J., Donaldson, K., 2016. The in vitro respiratory toxicity of cristobalite-bearing volcanic ash. Environ. Res. 145, 74–84. https://doi.org/10.1016/j.envres.2015.11.020.

Damby, D.E., Horwell, C.J., Larsen, G., Thordarson, T., Tomatis, M., Fubini, B., et al., 2017. Assessment of the potential respiratory hazard of volcanic ash from future Icelandic eruptions: a study of archived basaltic to rhyolitic ash samples. Environ. Health 16. https://doi.org/10.1186/s12940-017-0302-9.

Damby, D.E., Horwell, C.J., Baxter, P.J., Kueppers, U., Schnurr, M., Dingwell, D.B., et al., 2018. Volcanic ash activates the NLRP3 inflammasome in murine and human macrophages. Front. Immunol. 8, 2000. https://doi.org/10.3389/fimmu.2017.02000.

De Hoog, J., Koetsier, G., Bronto, S., Sriwana, T., Van Bergen, M., 2001. Sulfur and chlorine degassing from primitive arc magmas: temporal changes during the 1982–1983 eruptions of Galunggung (West Java, Indonesia). J. Volcanol. Geotherm. Res. 108 (1), 55–83. https://doi.org/10.1016/S0377-0273(00)00278-X.

de Moor, J.M., Fischer, T.P., Hilton, D.R., Hauri, E., Jaffe, L.A., Camacho, J.T., 2005. Degassing at Anatahan volcano during the May 2003 eruption: implications from petrology, ash leachates, and SO2 emissions. J. Volcanol. Geotherm. Res. 146 (1–3), 117–138. https://doi.org/10.1016/j.jvolgeores.2004.11.034.

Delmelle, P., Lambert, M., Dufrene, Y., Gerin, P., Oskarsson, N., 2007. Gas/aerosol-ash interaction in volcanic plumes: new insights from surface analyses of fine ash particles. Earth Planet. Sci. Lett. 259 (1–2), 159–170. https://doi.org/10.1016/j.epsl.2007.04.052.

Delmelle, P., Wadsworth, F.B., Maters, E.C., Ayris, P.M., 2018. High temperature reactions between gases and ash particles in volcanic eruption plumes. Rev. Mineral. Geochem. 84 (1), 285–308. https://doi.org/10.2138/rmg.2018.84.8.

Donaldson, K., Stone, V., Borm, P.J., Jimenez, L.A., Gilmour, P.S., Schins, R.P., et al., 2003. Oxidative stress and calcium signaling in the adverse effects of environmental particles (PM10). Free Radic. Biol. Med. 34 (11), 1369–1382. https://doi.org/10.1016/s0891-5849(03)00150-3.

Dopp, E., Yadav, S., Ansari, F.A., Bhattacharya, K., Von Recklinghausen, U., Rauen, U., et al., 2005. ROS-mediated genotoxicity of asbestos-cement in mammalian lung cells in vitro. Part. Fibre Toxicol. 2 (1), 9. https://doi.org/10.1186/1743-8977-2-9.

Fubini, B., 1997. Surface reactivity in the pathogenic response to particulates. Environ. Health Perspect. 105 (Suppl. 5), 1013. https://doi.org/10.1289/ehp.97105s51013.

Fubini, B., Mollo, L., Giamello, E., 1995. Free radical generation at the solid/liquid interface in iron containing minerals. Free Radic. Res. 23 (6), 593–614. https://doi.org/10.3109/10715769509065280.

Geh, S., Yücel, R., Duffin, R., Albrecht, C., Borm, P.J., Armbruster, L., et al., 2006. Cellular uptake and cytotoxic potential of respirable bentonite particles with different quartz contents and chemical modifications in human lung fibroblasts. Arch. Toxicol. 80 (2), 98–106. https://doi.org/10.1007/s00204-005-0013-9.

Ghiazza, M., Polimeni, M., Fenoglio, I., Gazzano, E., Ghigo, D., Fubini, B., 2010. Does vitreous silica contradict the toxicity of the crystalline silica paradigm? Chem. Res. Toxicol. 23 (3), 620–629. https://doi.org/10.1021/tx900369x.

Gilmour, P.S., Brown, D.M., Lindsay, T.G., Beswick, P.H., MacNee, W., Donaldson, K., 1996. Adverse health effects of PM10 particles: involvement of iron in generation of hydroxyl radical. Occup. Environ. Med. 53 (12), 817–822. https://doi.org/10.1136/oem.53.12.817.

Gislason, S.R., Hassenkam, T., Nedel, S., Bovet, N., Eiriksdottir, E.S., Alfredsson, H.A., et al., 2011. Characterization of Eyjafjallajökull volcanic ash particles and a protocol for rapid risk assessment. Proc. Natl. Acad. Sci. U. S. A 108 (18), 7307–7312. https://doi.org/10.1073/pnas.1015053108.

Gudmundsson, M.T., Thordarson, T., Hoskuldsson, A., Larsen, G., Bjornsson, H., Prata, F.J., et al., 2012. Ash generation and distribution from the April-May 2010 eruption of Eyjafjallajökull, Iceland. Sci. Rep. 2. https://doi.org/10.1038/srep00572.

Hansell, A.L., Horwell, C.J., Oppenheimer, C., 2006. The health hazards of volcanoes and geothermal areas. Occup. Environ. Med. 63 (2), 149–156. https://doi.org/10.1136/oem.2005.022459.

Hillman, S.E., Horwell, C.J., Densmore, A.L., Damby, D.E., Fubini, B., Ishimine, Y., et al., 2012. Sakurajima volcano: a physico-chemical study of the health consequences of long-term exposure to volcanic ash. Bull. Volcanol. 74 (4), 913–930. https://doi.org/10.1007/s00445-012-0575-3.

Hincks, T., Aspinall, W., Baxter, P., Searl, A., Sparks, R., Woo, G., 2006. Long term exposure to respirable volcanic ash on Montserrat: a time series simulation. Bull. Volcanol. 68 (3), 266–284. https://doi.org/10.1007/s00445-005-0006-9.

Horwell, C.J., Baxter, P.J., 2006. The respiratory health hazards of volcanic ash: a review for volcanic risk mitigation. Bull. Volcanol. 69 (1), 1–24. https://doi.org/10.1007/s00445-006-0052-y.

Horwell, C.J., Fenoglio, I., Fublni, B., 2007. Iron-induced hydroxyl radical generation from basaltic volcanic ash. Earth Planet. Sci. Lett. 261 (3–4), 662–669. https://doi.org/10.1016/j.epsl.2007.07.032.

Horwell, C.J., Baxter, P.J., Hillman, S.E., Calkins, J.A., Damby, D.E., Delmelle, P., et al., 2013. Physicochemical and toxicological profiling of ash from the 2010 and 2011 eruptions of Eyjafjallajökull and Grímsvötn volcanoes, Iceland using a rapid respiratory hazard assessment protocol. Environ. Res. 127, 63–73. https://doi.org/10.1016/j.envres.2013.08.011.

Horwell, C.J., Fenoglio, I., Ragnarsdottir, K.V., Sparks, R.S.J., Fubini, B., 2003. Surface reactivity of volcanic ash from the eruption of Soufrière Hills volcano, Montserrat, West Indies with implications for health hazards. Environ. Res. 93 (2), 202–215. https://doi.org/10.1016/s0013-9351(03)00044-6.

Horwell, C.J., Sparks, R.S.J., Brewer, T.S., Llewellin, E.W., Williamson, B.J., 2003. Characterization of respirable volcanic ash from the Soufrière Hills volcano, Montserrat, with implications for human health hazards. Bull. Volcanol. 65 (5), 346–362. https://doi.org/10.1007/s00445-002-0266-6.

Horwell, C.J., Williamson, B.J., Le Blond, J.S., Donaldson, K., Damby, D.E., Bowen, L., 2012. The structure of volcanic cristobalite in relation to its toxicity; relevance for the variable crystalline silica hazard. Part. Fibre Toxicol. 9, 44. https://doi.org/10.1186/1743-8977-9-44.

Hoshyaripour, G., Hort, M., Langmann, B., Delmelle, P., 2014. Volcanic controls on ash

iron solubility: new insights from high-temperature gas–ash interaction modeling. J. Volcanol. Geotherm. Res. 286, 67–77. https://doi.org/10.1016/j.jvolgeores.2014.09.005.
Kar-Purkayastha, I., Horwell, C., Murray, V., 2012. Review of Evidence on the Potential Health Impacts of Volcanic Ash on the Population of the UK and ROI. Health Protection Agency, London ISBN 978-0-85951-733-1.
Könczöl, M., Goldenberg, E., Ebeling, S., Schäfer, B., Garcia-Käufer, M., Gminski, R., et al., 2012. Cellular uptake and toxic effects of fine and ultrafine metal-sulfate particles in human A549 lung epithelial cells. Chem. Res. Toxicol. 25 (12), 2687–2703. https://doi.org/10.1021/tx300333z.
Lahde, A., Gudmundsdottir, S.S., Joutsensaari, J., Tapper, U., Ruusunen, J., Ihalainen, M., et al., 2013. In vitro evaluation of pulmonary deposition of airborne volcanic ash. Atmos. Environ. 70, 18–27. https://doi.org/10.1016/j.atmosenv.2012.12.048.
Le Blond, J.S., Horwell, C.J., Baxter, P.J., Michnowicz, S.A.K., Tomatis, M., Fubini, B., et al., 2010. Mineralogical analyses and in vitro screening tests for the rapid evaluation of the health hazard of volcanic ash at Rabaul volcano, Papua New Guinea. Bull. Volcanol. 72 (9), 1077–1092. https://doi.org/10.1007/s00445-010-0382-7.
Lee, S.H., Richards, R.J., 2004. Montserrat volcanic ash induces lymph node granuloma and delayed lung inflammation. Toxicology 195 (2–3), 155–165. https://doi.org/10.1016/j.tox.2003.09.013.
Lenz, A.G., Karg, E., Lentner, B., Dittrich, V., Brandenberger, C., Rothen-Rutishauser, B., et al., 2009. A dose-controlled system for air-liquid interface cell exposure and application to zinc oxide nanoparticles. Part. Fibre Toxicol. 6. https://doi.org/10.1186/1743-8977-6-32.
Maters, E.C., Delmelle, P., Rossi, M.J., Ayris, P.M., Bernard, A., 2016. Controls on the surface chemical reactivity of volcanic ash investigated with probe gases. Earth Planet. Sci. Lett. 450, 254–262. https://doi.org/10.1016/j.epsl.2016.06.044.
Maters, E.C., Delmelle, P., Rossi, M.J., Ayris, P.M., 2017. Reactive uptake of sulfur dioxide and ozone on volcanic glass and ash at ambient temperature. J. Geophys. Res.: Atmos. 122 (18). https://doi.org/10.1002/2017JD026993.
Monick, M.M., Baltrusaitis, J., Powers, L.S., Borcherding, J.A., Caraballo, J.C., Mudunkotuwa, I., et al., 2013. Effects of Eyjafjallajökull volcanic ash on innate immune system responses and bacterial growth in vitro. Environ. Health Perspect. 121 (6), 691–698. https://doi.org/10.1289/ehp.1206004.
Moss, O., 1979. Simulants of lung interstitial fluid. Health Phys. 36 (3), 447–448.
Mueller, S.B., Ayris, P.M., Wadsworth, F.B., Kueppers, U., Casas, A.S., Delmelle, P., et al., 2017. Ash aggregation enhanced by deposition and redistribution of salt on the surface of volcanic ash in eruption plumes. Sci. Rep. 7. https://doi.org/10.1038/srep45762.
Nattrass, C., Horwell, C.J., Damby, D.E., Brown, D., Stone, V., 2017. The effect of aluminium and sodium impurities on the cytotoxicity and pro-inflammatory potential of cristobalite. Environ. Res. 159C, 164–175. https://doi.org/10.1016/j.envres.2017.07.054.
Olsson, J., Stipp, S.L.S., Dalby, K.N., Gislason, S., 2013. Rapid release of metal salts and nutrients from the 2011 Grímsvötn, Iceland volcanic ash. Geochem. Cosmochim. Acta 123, 134–149. https://doi.org/10.1016/j.gca.2013.09.009.
Oskarsson, N., 1980. The interaction between volcanic gases and tephra - fluorine adhering to tephra of the 1970 Hekla eruption. J. Volcanol. Geotherm. Res. 8 (2–4), 251–266. https://doi.org/10.1016/0377-0273(80)90107-9.
Parkhurst, D.L., Appelo, C., 2013. Description of Input and Examples for PHREEQC Version 3 - A Computer Program for Speciation, Batch-Reaction, One-Dimensional Transport, and Inverse Geochemical Calculations. U.S. Geological Survey Techniques and Methods, Chapter A43, Book 6.
Paul, D., Achouri, S., Yoon, Y.-Z., Herre, J., Bryant, C.E., Cicuta, P., 2013. Phagocytosis dynamics depends on target shape. Biophys. J. 105 (5), 1143–1150. https://doi.org/10.1016/j.bpj.2013.07.036.
Pinkerton, K.E., Gehr, P., Castañeda, A., Crapo, J.D., 2015. Architecture and Cellular Composition of the Air–Blood Tissue Barrier. Comparative Biology of the Normal Lung. Elsevier, pp. 105–117.
Renggli, C.J., King, P.L., 2018. $SO_2$ gas reactions with silicate glasses. Rev. Mineral. Geochem. 84 (1), 229–255. https://doi.org/10.2138/rmg.2018.84.6.
Rice, T.M., Clarke, R.W., Godleski, J.J., Al-Mutairi, E., Jiang, N.-F., Hauser, R., et al., 2001. Differential ability of transition metals to induce pulmonary inflammation. Toxicol. Appl. Pharmacol. 177 (1), 46–53. https://doi.org/10.1006/taap.2001.9287.
Romani, A.M., 2011. Cellular magnesium homeostasis. Arch. Biochem. Biophys. 512 (1), 1–23. https://doi.org/10.1016/j.abb.2011.05.010.
Romani, A., Scarpa, A., 2000. Regulation of cellular magnesium. Front. Biosci. 5 (1), D720–D734. https://doi.org/10.2741/romani.
Rose, W.I., 1977. Scavenging of volcanic aerosol by ash: Atmospheric and volcanologic implications. Geology 5 (10), 621–624. https://doi.org/10.1130/0091-7613(1977)5<621:sovaba>2.0.co;2.
Rose, W., Bonis, S., Stoiber, R., Keller, M., Bickford, T., 1973. Studies of volcanic ash from two recent Central American eruptions. Bull. Volcanol. 37 (3), 338–364. https://doi.org/10.1007/BF02597633.
Rothen-Rutishauser, B.M., Kiama, S.G., Gehr, P., 2005. A three-dimensional cellular model of the human respiratory tract to study the interaction with particles. Am. J. Respir. Cell Mol. Biol. 32 (4), 281–289. https://doi.org/10.1165/rcmb.2004-0187OC.
Rothen-Rutishauser, B., Mueller, L., Blank, F., Brandenberger, C., Muehlfeld, C., Gehr, P., 2008. A newly developed in vitro model of the human epithelial airway barrier to study the toxic potential of nanoparticles. Altex Altern. Zu Tierexperimenten. 25 (3), 191–196.
Schorn, C., Frey, B., Lauber, K., Janko, C., Strysio, M., Keppeler, H., et al., 2011. Sodium overload and water influx activate the NALP3 inflammasome. J. Biol. Chem. 286 (1), 35–41. https://doi.org/10.1074/jbc.M110.139048.
Searl, A., Nicholl, A., Baxter, P., 2002. Assessment of the exposure of islanders to ash from the Soufrière Hills volcano, Montserrat, British West Indies. Occup. Environ. Med. 59 (8), 523–531. https://doi.org/10.1136/oem.59.8.523.
Smith, D.B., Zielinski, R.A., Rose, W.I., Huebert, B.J., 1982. Water-soluble material on aerosols collected within volcanic eruption clouds. J. Geophys. Res. Ocean. 87 (NC7), 4963–4972. https://doi.org/10.1029/JC087iC07p04963.
Smith, D., Zielinski, R., Taylor, H., Sawyer, M., 1983. Leaching characteristics of ash from the May 18, 1980, eruption of Mount St. Helens volcano, Washington. Bull. Volcanol. 46 (2), 103–124. https://doi.org/10.1007/BF02597580.
Smith, K.R., Veranth, J.M., Hu, A.A., Lighty, J.S., Aust, A.E., 2000. Interleukin-8 levels in human lung epithelial cells are increased in response to coal fly ash and vary with the bioavailability of iron, as a function of particle size and source of coal. Chem. Res. Toxicol. 13 (2), 118–125. https://doi.org/10.1021/tx9901736.
Steiner, S., Czerwinski, J., Comte, P., Mueller, L.L., Heeb, N.V., Mayer, A., et al., 2013. Reduction in (pro-)inflammatory responses of lung cells exposed in vitro to diesel exhaust treated with a non-catalyzed diesel particle filter. Atmos. Environ. 81, 117–124. https://doi.org/10.1016/j.atmosenv.2013.08.029.
Stewart, C., Horwell, C.J., Plumlee, G., Cronin, S., Delmelle, P., Baxter, P., Calkins, J., Damby, D.E., Morman, S., Oppenheimer, C., 2013. Protocol for analysis of volcanic ash samples for assessment of hazards from leachable elements. IAVCEI Commissions Joint Report International Volcanic Health Hazard Network and Cities and Volcanoes. IVHHN, pp. 21. http://www.ivhhn.org/guidelines.html.
Taylor, P.S., Stoiber, R.E., 1973. Soluble material on ash from active Central American volcanoes. Geol. Soc. Am. Bull. 84 (3), 1031–1041. https://doi.org/10.1130/0016-7606(1973)84<1031:smoafa>2.0.co;2.
Tomašek, I., Horwell, C.J., Damby, D.E., Barošová, H., Geers, C., Petri-Fink, A., et al., 2016. Combined exposure of diesel exhaust particles and respirable Soufrière Hills volcanic ash causes a (pro-)inflammatory response in an in vitro multicellular epithelial tissue barrier model. Part. Fibre Toxicol. 13 (1), 67. https://doi.org/10.1186/s12989-016-0178-9.
Tomašek, I., Horwell, C.J., Bisig, C., Damby, D.E., Comte, P., Czerwinski, J., et al., 2018. Respiratory hazard assessment of combined exposure to complete gasoline exhaust and respirable volcanic ash in a multicellular human lung model at the air-liquid interface. Environ. Pollut. 238, 977–987. https://doi.org/10.1016/j.envpol.2018.01.115.
Wilson, M.R., Stone, V., Cullen, R.T., Searl, A., Maynard, R.L., Donaldson, K., 2000. In vitro toxicology of respirable Montserrat volcanic ash. Occup. Environ. Med. 57 (11), 727–733. https://doi.org/10.1136/oem.57.11.727.
Witham, C.S., Oppenheimer, C., Horwell, C.J., 2005. Volcanic ash-leachates: a review and recommendations for sampling methods. J. Volcanol. Geotherm. Res. 141 (3–4), 299–326. https://doi.org/10.1016/j.jvolgeores.2004.11.010.
Yang, N.J., Hinner, M.J., 2015. Getting Across the Cell Membrane: An Overview for Small Molecules, Peptides, and Proteins. In: Gautier, A., Hinner, M. (Eds.), Site-Specific Protein Labeling. Methods in Molecular Biology. Springer, pp. 29–53 1266.